Detection of elemental mercury by multimode diode laser correlation spectroscopy

Lou, Xiutao; Somesfalean, Gabriel; Svanberg, Sune; Zhang, Zhiguo; Wu, Shaohua

Published in:
Optics Express

DOI:
10.1364/OE.20.004927

2012

Detection of elemental mercury by multimode diode laser correlation spectroscopy

Xiutao Lou,[1,2,4] Gabriel Somesfalean,[2,3,5] Sune Svanberg,[2,3] Zhiguo Zhang,[1,6] and Shaohua Wu[4]

[1]*Department of Physics, Harbin Institute of Technology, Harbin 150001, China*
[2]*Department of Physics, Lund University, Lund 22100, Sweden*
[3]*Joint Research Center of Photonics, Zhejiang University-Royal Institute of Technology-Lund University, Hangzhou 310058, China*
[4]*Institute of Combustion Engineering, Harbin Institute of Technology, Harbin 150001, China*
[5]*gabriels@fysik.lth.se*
[6]*zhangzhiguo@hit.edu.cn*

Abstract: We demonstrate a method for elemental mercury detection based on correlation spectroscopy employing UV laser radiation generated by sum-frequency mixing of two visible multimode diode lasers. Resonance matching of the multimode UV laser is achieved in a wide wavelength range and with good tolerance for various operating conditions. Large mode-hops provide an off-resonance baseline, eliminating interferences from other gas species with broadband absorption. A sensitivity of 1 μg/m^3 is obtained for a 1-m path length and 30-s integration time. The performance of the system shows promise for mercury monitoring in industrial applications.

OCIS codes: (140.2020) Diode lasers; (140.3600) Lasers, tunable; (300.1030) Absorption; (300.6210) Spectroscopy, atomic.

References and links

1. U.S. Environmental Protection Agency, "Mercury study report to congress, Vol. I: Executive Summary," EPA-452/R-97–003 (December, 1997).
2. http://www.epa.gov/CAMR/.
3. Ministry of Environmental Protection of China, "Emission standard of air pollutants for thermal power plants," GB13223–2011 (July, 2011).
4. J. H. Pavlish, E. A. Sondreal, M. D. Mann, E. S. Olson, K. C. Galbreath, D. L. Laudal, and S. A. Benson, "Status review of mercury control options for coal-fired power plants," Fuel Process. Technol. **82**(2-3), 89–165 (2003).
5. D. L. Laudal, J. S. Thompson, J. H. Pavlish, L. A. Brickett, and P. Chu, "Use of continuous mercury monitors at coal-fired utilities," Fuel Process. Technol. **85**(6-7), 501–511 (2004).
6. S. Sholupov, S. Pogarev, V. Ryzhov, N. Mashyanov, and A. Stroganov, "Zeeman atomic absorption spectrometer RA-915+ for direct determination of mercury in air and complex matrix samples," Fuel Process. Technol. **85**(6-7), 473–485 (2004).
7. T. Hadeishi, D. A. Church, R. D. McLaughlin, B. D. Zak, M. Nakamura, and B. Chang, "Mercury monitor for ambient air," Science **187**(4174), 348–349 (1975).
8. H. Edner, A. Sunesson, S. Svanberg, L. Unéus, and S. Wallin, "Differential optical absorption spectroscopy system used for atmospheric mercury monitoring," Appl. Opt. **25**(3), 403–409 (1986).
9. E. D. Thoma, C. Secrest, E. S. Hall, D. Lee Jones, R. C. Shores, M. Modrak, R. Hashmonay, and P. Norwood, "Measurement of total site mercury emissions from a chlor-alkali plant using ultraviolet differential optical absorption spectroscopy and cell room roof-vent monitoring," Atmos. Environ. **43**(3), 753–757 (2009).
10. J. Alnis, U. Gustafsson, G. Somesfalean, and S. Svanberg, "Sum-frequency generation with a blue diode laser for mercury spectroscopy at 254 nm," Appl. Phys. Lett. **76**(10), 1234–1236 (2000).
11. A. E. Carruthers, T. K. Lake, A. Shah, J. W. Allen, W. Sibbett, and K. Dholakia, "Single-scan spectroscopy of mercury at 253.7 nm by sum frequency mixing of violet and red microlensed diode lasers," Opt. Commun. **255**(4-6), 261–266 (2005).
12. T. N. Anderson, J. K. Magnuson, and R. P. Lucht, "Diode-laser-based sensor for ultraviolet absorption measurements of atomic mercury," Appl. Phys. B **87**(2), 341–353 (2007).
13. R. Wallenstein and T. W. Hänsch, "Powerful dye laser oscillator-amplifier system for high resolution spectroscopy," Opt. Commun. **14**(3), 353–357 (1975).
14. M. Aldén, H. Edner, and S. Svanberg, "Remote measurement of atmospheric mercury using differential absorption lidar," Opt. Lett. **7**(5), 221–223 (1982).

#160551 - $15.00 USD Received 3 Jan 2012; revised 3 Feb 2012; accepted 3 Feb 2012; published 13 Feb 2012

15. M. Sjöholm, P. Weibring, H. Edner, and S. Svanberg, "Atomic mercury flux monitoring using an optical parametric oscillator based lidar system," Opt. Express **12**(4), 551–556 (2004).
16. J. Paul, Y. Kaneda, T. L. Wang, C. Lytle, J. V. Moloney, and R. J. Jones, "Doppler-free spectroscopy of mercury at 253.7 nm using a high-power, frequency-quadrupled, optically pumped external-cavity semiconductor laser," Opt. Lett. **36**(1), 61–63 (2011).
17. M. Scheid, F. Markert, J. Walz, J. Y. Wang, M. Kirchner, and T. W. Hänsch, "750 mW continuous-wave solid-state deep ultraviolet laser source at the 253.7 nm transition in mercury," Opt. Lett. **32**(8), 955–957 (2007).
18. G. Somesfalean, M. Sjoholm, L. Persson, H. Gao, T. Svensson, and S. Svanberg, "Temporal correlation scheme for spectroscopic gas analysis using multimode diode lasers," Appl. Phys. Lett. **86**(18), 184102 (2005).
19. X. T. Lou, G. Somesfalean, and Z. G. Zhang, "Gas detection by correlation spectroscopy employing a multimode diode laser," Appl. Opt. **47**(13), 2392–2398 (2008).
20. X. T. Lou, G. Somesfalean, B. Chen, Y. G. Zhang, H. S. Wang, Z. G. Zhang, S. H. Wu, and Y. K. Qin, "Simultaneous detection of multiple-gas species by correlation spectroscopy using a multimode diode laser," Opt. Lett. **35**(11), 1749–1751 (2010).
21. M. L. Huber, A. Laesecke, and D. G. Friend, "Correlation for the vapor pressure of mercury," Ind. Eng. Chem. Res. **45**(21), 7351–7361 (2006).
22. P. Werle, "Accuracy and precision of laser spectrometers for trace gas sensing in the presence of optical fringes and atmospheric turbulence," Appl. Phys. B **102**(2), 313–329 (2011).
23. Y. Nishimura and T. Fujimoto, "λ=2537 Å line from a low-pressure mercury discharge lamp emission profile and line absorption by a gas containing a mercury-vapor," Appl. Phys. B **38**(2), 91–98 (1985).
24. A. C. Vandaele, C. Hermans, and S. Fally, "Fourier transform measurements of SO(2) absorption cross sections: II. Temperature dependence in the 29 000-44 000 cm(–1) (227-345 nm) region," J. Quant. Spectrosc. Radiat. Transf. **110**(18), 2115–2126 (2009).

1. Introduction

Mercury is an important pollutant due to its bioaccumulation as methylmercury and its neurological health impacts. The amount of mercury mobilized into the biosphere has increased due to human activities. Most of the anthropogenic emissions of mercury come from combustion sources, especially coal-fired utilities [1]. Many countries have issued regulations to control the mercury emissions from coal-fired power plants [2, 3], e.g., China has recently established a mercury emission limit of 30 $\mu g/m^3$ for coal-fired boilers [3]. Corresponding mercury removal technologies are continuously developed [4]. These mercury control requirements call for effective measurement techniques.

Mercury is present in elemental or oxidized states in industrial exhaust. Currently, the conventional methods in terms of sensitivity and accuracy are the wet-chemistry procedures, e.g. EPA 29 and EPA 101A for total mercury, and the Ontario Hydro method for speciated mercury. Although these methods can achieve a high level of sensitivity (<0.5 $\mu g/m^3$) [5], they require expert operation and are time consuming. Therefore, automated continuous emission monitors (CEMs) are being developed [5]. The oxidized mercury is converted to elemental mercury by a wet-chemistry or thermal conversion unit, then the total or speciated mercury concentration is determined by atomic absorption spectroscopy or fluorescence. Most CEMs utilize a preconcentration step to collect mercury and remove interference species such as SO_2 and NO_X, which, however, significantly slows down the response time of the system. Only a few CEMs dispense with a preconcentration unit, since they utilize optical techniques which can discriminate against interfering impurities, e.g. Zeeman-modulated atomic absorption spectroscopy (ZAAS) [6, 7] and differential optical absorption spectroscopy (DOAS) [8, 9]. Both ZAAS and DOAS employ the mercury absorption lines around 253.7 nm, thus being able to simultaneously and readily record on- and off- resonance signals. Typical sensitivities of current commercial CEMs for mercury emission monitoring are around 0.5 $\mu g/m^3$ [6].

An alternative technique for elemental mercury detection is the employment of laser absorption spectroscopy. Various techniques have been developed to generate laser radiation at 253.7 nm, including sum-frequency generation (SFG) by two diode lasers (DLs) [10–12], frequency doubling pulsed dye lasers or optical-parametric-oscillator lasers [13–15] and frequency quadrupling diode lasers or solid-state lasers [16, 17]. By comparison, SFG-DL based systems possess the merits of agile tunability, simplicity and low-cost. Diode-laser-based systems with mode-hop-free tuning in the range of 35-100 GHz have previously been

#160551 - $15.00 USD Received 3 Jan 2012; revised 3 Feb 2012; accepted 3 Feb 2012; published 13 Feb 2012

developed [10–12]. For mercury sensing by tunable diode laser absorption spectroscopy (TDLAS) two requirements should be fulfilled: extremely accurate wavelength control and wide mode-hop free tuning range (> 80 GHz). These are either difficult to achieve in real-world applications or time-consuming.

In this paper, we demonstrate mercury sensing by multimode diode laser correlation spectroscopy (MDL-COSPEC) [18–20]. A multimode UV laser centered at 253.7 nm is generated by sum-frequency mixing of a low-cost violet MDL and a Fabry-Pérot (FP) type quasi-single-mode red DL. Mercury absorption is readily obtained for a wide setting of multimodes, yielding the system good tolerance to variations in the laser operation temperature and current. The MDL-COSPEC technique operates more reliable compared with the TDLAS, illustrated by the use of a varying and broad spectral multimode 'comb' rather than a demanding and fine single-mode 'needle' to interact with the sharp absorption line of a gas. Furthermore, large off-resonant mode-hops provide a baseline, thus effectively eliminating interferences from other gas species and light intensity fluctuations. Wavelength modulation spectroscopy (WMS), as a general sensitive-enhancing technique, was also utilized in this work. The system was evaluated in terms of quantitative analysis performance, sensitivity, selectivity and tolerance to wavelength change.

2. Experimental setup

The experimental setup for sum-frequency generation and multimode diode laser correlation spectroscopy is schematically shown in Fig. 1. The multimode UV radiation around 253.7 nm is generated by sum-frequency mixing of a FP type violet diode laser (Libao Laser, 405 nm, 50 mW) with a FP type red diode laser (SDL Inc., 677 nm, 30 mW) in a Beta-Barium-Borate (BBO) crystal (Caston Optronics).

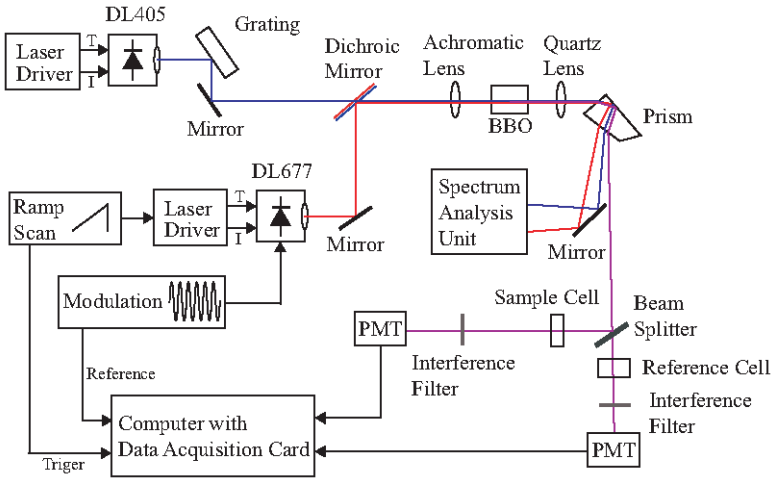

Fig. 1. Diagram of the MDL-COSPEC-based elemental mercury detection system.

The free-running emission of the violet diode laser includes more than 20 longitudinal modes, as shown in Fig. 2. Since laser modes non-interacting with the gas can dilute the magnitude of the absorption signal, in order to increase the magnitude of the absorption signal, only a few modes (< 5) are selected by using a Littrow-type cavity equipped with a 2400 l/mm grating. The red diode laser operates in a quasi-single-mode emission with frequent mode-hops, i.e., its emission consists of a dominant mode and several minor side modes. as shown in Fig. 3. A closer look at the figure reveals that the laser wavelength at the whole increases with the increase of laser current, which is due to a shift of the gain curve towards higher wavelengths with increased laser chip temperature. On the other hand, because of mode hops the laser

#160551 - $15.00 USD Received 3 Jan 2012; revised 3 Feb 2012; accepted 3 Feb 2012; published 13 Feb 2012

wavelength can “jump” back and forth when the laser current changes, which can result in temporary lower wavelength at higher laser currents.

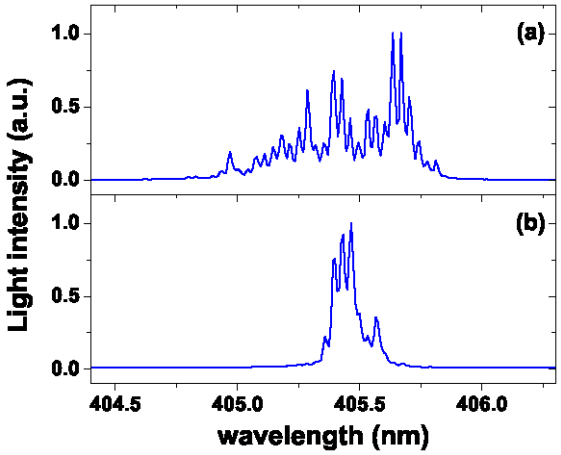

Fig. 2. Typical emission spectra of the violet diode laser operated at 33 °C and 110 mA (a) in free running condition and (b) with external grating feedback.

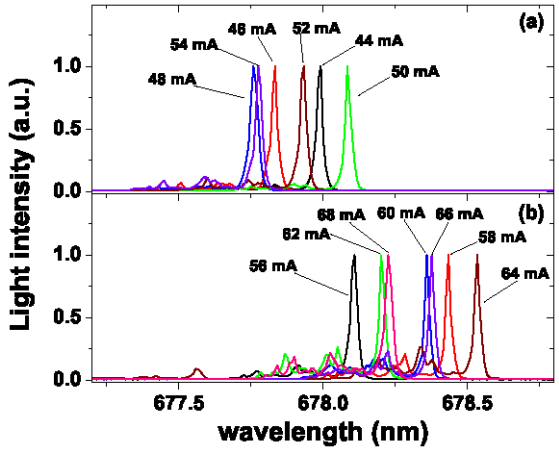

Fig. 3. Emission spectra of the red diode laser employed with 32 °C operating temperature at different operating currents: (a) 44-54 mA and (b) 56-68 mA.

The violet and the red beams are spatially overlapped by a dichroic mirror and focused into a 7-mm-long BBO crystal by an $f = 40$ mm achromatic lens. The BBO crystal is cut at $\theta = 48.9°$ and slightly tilted to achieve Type I phase matching. The UV light exiting the crystal is collimated by an $f = 40$ mm quartz lens and separated from the fundamental radiation by a Pellin-Broca prism. The fundamental violet and red laser beams are directed into a spectrum analyser unit comprised of a grating spectrometer (Jobin Yvon) and a spectrum analyzer (Tropel Model 240). The generated UV light is split by a 50/50 beam splitter into two beams passing through a 6-mm reference cell and a 4-mm sample cell, respectively. Both cells are filled with mercury vapor at atmospheric pressure and room temperature. The number density of the mercury vapor can be calculated according to the liquid-mercury temperature [21]. The reference UV beam is detected by a photomultiplier (PMT, EMI 9592B) combined with a 254 ± 10 nm interference filter having a transmission of 14.5%, while the sample beam is detected by another PMT (EMI 9817Q) combined with a 254 ± 10 nm interference filter having a

#160551 - $15.00 USD Received 3 Jan 2012; revised 3 Feb 2012; accepted 3 Feb 2012; published 13 Feb 2012

transmission of 1.4%.The signals from both PMTs are collected by a data acquisition card (PCI-6132, National Instruments).

The SFG UV light power is estimated to be 2 nW by comparison with the attenuated UV light from an LED (with a center wavelength of 255 nm and full width at half maximum of 10 nm). The light power of the LED is evaluated by using a Si photodiode having a responsivity of 0.04 A/W around 255 nm. The violet and red laser powers entering the BBO crystal are measured to be 11 mW and 25 mW, respectively. From theoretical calculations, one order of magnitude larger UV power could be obtained by decreasing the laser spot size in the crystal [10]. However, no such attempts were made since it would increase the system sensitivity to vibrations, thus degrading the system stability.

The absorption signals of mercury are obtained by ramp sweeping the red laser from 44 to 68 mA at 8 Hz repetition rate. The grating spectrometer having an accuracy of 0.2 nm is employed to check the center wavelengths of the lasers. The center wavelength of the violet laser is set to 405.5 nm by adjusting the grating angle of the external cavity. In order to increase the output laser power, the center wavelength of the laser gain curve is also adjusted to 405.5 nm by tuning the laser temperature to 33 °C. The center of the wavelength scanning range of the red laser is tuned to 678 nm by setting its temperature to 32 °C. For measurement of the direct absorption signals, the current signals from the PMTs are converted into voltage signals by using 200-kΩ-load resistors and acquired by a data acquisition card (PCI-6132, National Instruments). To implement WMS, where a high detection bandwidth is required, transimpedance amplifiers (C7319, Hamamatsu) are employed instead of resistors. An 8 kHz sine wave is coupled to the diode laser to perform frequency modulation, and the signals are demodulated at 2*f* (i.e., 16 kHz) of the modulation frequency.

3. Measurement and analysis

Figure 4(a) shows typical raw signals from the sample and the reference channels with 80 scans averaged. Both the sample and reference mercury vapor concentrations are 19.1 ± 0.2 μg/m^3. After normalization to the baseline, i.e., to the initial light intensity without absorption, the direct absorption signals obtained are shown in Fig. 4(b). It can be seen that the line profiles of the absorption signals have sharp edges being neither Gaussian nor Lorenzian in shape, which is due to incomplete scans over part of the entire mercury absorption spectrum. The typical mode-hop-free tuning range of the red laser is measured to be less than 5 GHz and the mode-hops can change the laser frequency more than 100 GHz, which is larger than the frequency splitting of the isotope-shifted mercury vapor absorption spectrum (~25 GHz). This means that the recorded signals are generated when the laser frequency accidentally “jumps” into the absorption frequency region of mercury and scans a few GHz, then “jumps” out again to frequencies where mercury is not absorbing. Figure 4(c) shows the corresponding WMS-2f signals. The concentration of the sample gas can be obtained by employing the well-calibrated concentration of the reference gas and the magnitude ratio between the sample and the reference absorption signals.

#160551 - $15.00 USD Received 3 Jan 2012; revised 3 Feb 2012; accepted 3 Feb 2012; published 13 Feb 2012

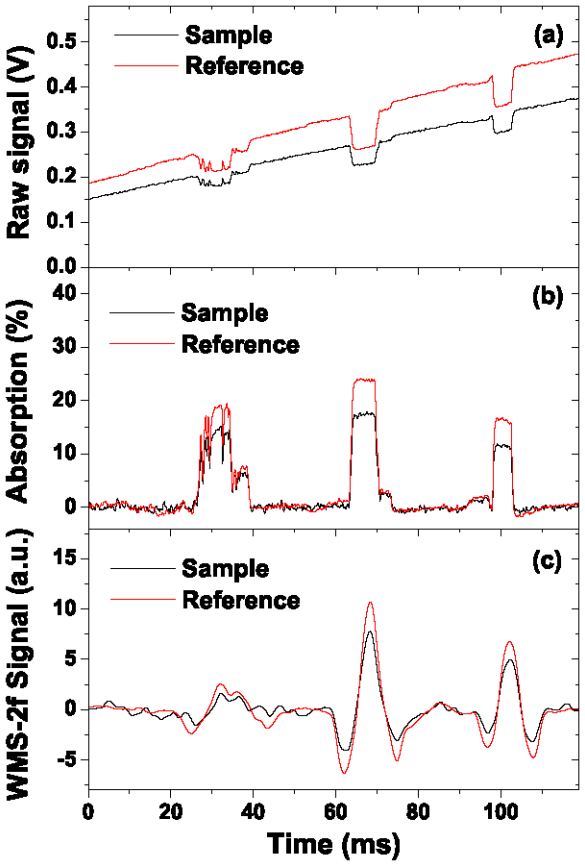

Fig. 4. Typical mercury absorption signal pairs with 80 scans averaged: (a) Raw signals recorded by a DAQ card. (b) Direct absorption signals. (c) WMS-2f signals.

Since it is difficult to directly measure the generated multimode UV laser emission spectrum, a 20-mm-long mercury cell is utilized to yield 100% absorption for on-resonance radiation. Figure 5(a) shows that the absorption signals yield a maximum of around 40%. It indicates that the remaining ~60% of the laser intensity corresponds to modes which are not absorbed. In order to verify the frequent mode-hop behavior of the red DL shown in Fig. 3, thus verifying the mode-hop behavior of the resulting UV laser, a spectrum analyzer with a free spectral range of 1.5 GHz is employed. Figure 5(b) shows the obtained etalon signal during one ramp scan of the laser. The high finesse etalon fringes obtained mean that the laser mostly operates at nearly single mode. However, since the periodicity of the etalon signals is low, it indicates that the laser is subject to frequent mode hops and that the mode-hop-free range is less than 5 GHz. Figure 5(c) shows the UV light intensity within a ramp scan. It is worth noting that there are no obvious intensity fluctuations due to mode hops.

#160551 - $15.00 USD Received 3 Jan 2012; revised 3 Feb 2012; accepted 3 Feb 2012; published 13 Feb 2012

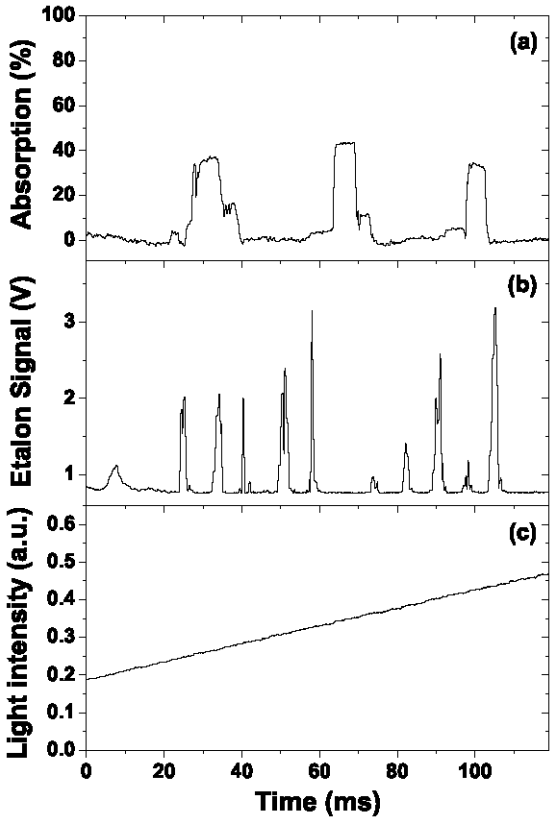

Fig. 5. (a) Absorption signals for a 20-mm mercury cell and (b) corresponding etalon signals of the red diode laser. (c) UV light intensity variation during a ramp scan.

4. Performance characterization

According to Figs. 4(b) and 4(c) and due to the large gas absorption recorded, it is currently of no advantage to use the WMS technique instead of direct detection. However, since WMS is a zero-background technique, which can increase the accuracy of the absorption signal evaluation, it is employed for the present mercury detection system.

4.1 Ability for quantitative analysis

In order to test the ability of the proposed elemental mercury detection system for quantitative analysis, five different concentrations of mercury vapor are measured. In order to achieve satisfactory SNR at low mercury vapor concentrations, a 20-mm cell is used here as the sample gas cell instead of the original 4-mm cell – which was used in all the other evaluation experiments. The mercury vapor concentration is controlled by adjusting the temperature in the cold finger of the gas cell. The recorded WMS signal magnitudes as a function of the mercury concentration are shown in Fig. 6. The WMS signal magnitude is defined here as the average peak-to-peak value of the WMS-2f signal (with both dips considered). The error bars represent plus and minus one standard deviation obtained for 10-minute-long successive measurements. The error bars mainly correspond to the shot noise and fluctuations of the gas temperature with an amplitude of ~0.3 °C. It can be noted that good linearity was obtained at lower concentrations, while for high gas concentrations a calibration curve can be employed to correct for the observed and expected non-linearity.

#160551 - $15.00 USD Received 3 Jan 2012; revised 3 Feb 2012; accepted 3 Feb 2012; published 13 Feb 2012

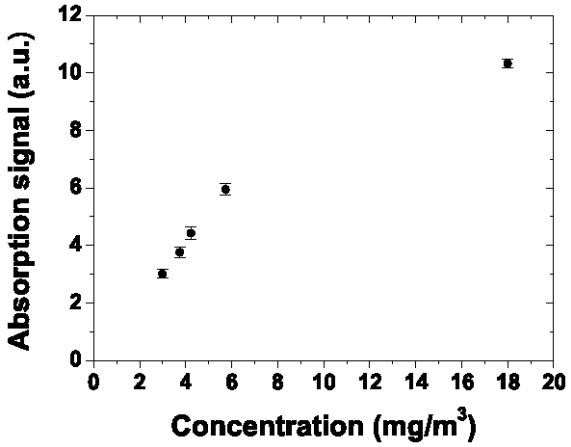

Fig. 6. Plots of mercury absorption signals as a function of concentration.

4.2 Sensitivity

For PMTs used for detection of low power light, the shot noise is the dominant noise source. Figure 4 shows that within a ramp scan different absorption signals not only have different magnitudes, but also different noise levels due to light intensity differences. Since the final concentration is retrieved from multiple absorption signals with different SNRs, the sensitivity of the proposed elemental mercury detection system based on MDL-COSPEC is evaluated by performing an Allan variance analysis [22] on continuous measurements. During an 80-minute measurement series, the room air temperature around the mercury cells is measured to be 24.2 ± 0.1 °C, with the corresponding mercury vapor concentration being 18.6 ± 0.2 μg/m^3. Figure 7 shows the Allan variance plot which indicates that a sensitivity of 1 μg/m^2 (concentration unit per integrated path length), i.e., 1 μg/m^3 for 1-m path length, can be achieved using a 30-s measurement time.

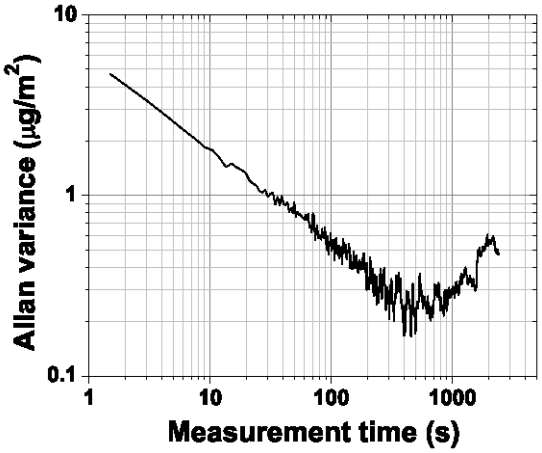

Fig. 7. Allan variance plot for an 80-min measurement series.

4.3 Selectivity

Laser absorption spectroscopy has intrinsic advantages regarding species selectivity. In order to evaluate the immunity of the system to interferences from other species, a 10-cm gas cell containing 2000 ppm of SO_2 is inserted into the sample optical path. The SO_2 is selected as a candidate interfering gas because it has a strong absorption around 254 nm and is frequently

#160551 - $15.00 USD Received 3 Jan 2012; revised 3 Feb 2012; accepted 3 Feb 2012; published 13 Feb 2012

present at high concentrations (typically hundreds to thousands of ppm) in coal combustion exhaust. Figure 8(a) shows the sample absorption signals of mercury vapor with and without the interfering SO_2 gas, and Fig. 8(b) shows the simultaneously recorded reference signals. The consistence of the sample signals shown in Fig. 8(a) indicates that the presence of SO_2 has no significant influence on the mercury detection. The slight signal discrepancy is mainly due to the wavelength and intensity changes of the laser modes between the different measurements, which is verified by the reference signals having the same signal discrepancy, as shown in Fig. 8(b).

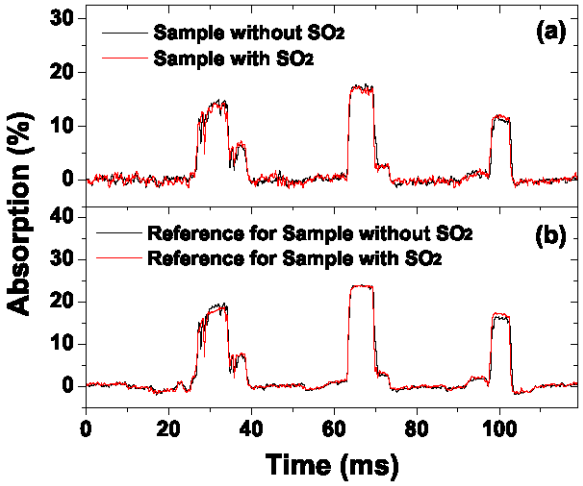

Fig. 8. (a) Sample absorption signals of mercury vapor with and without interference by SO_2 (2000 ppm, 10 cm) and (b) corresponding reference signals.

In order to further illustrate the selectivity as well as the sensitivity of the technique, we compare the absorption spectra of mercury vapor and SO_2 around 254 nm at atmospheric pressure by utilizing published spectroscopic data [23, 24]. The simulated spectra are shown in Fig. 9, where the optical path length for both gases is 1 m, the mercury vapor concentration is 1 $\mu g/m^3$ – which represents the sensitivity achieved in the present work – and the SO_2 concentration is 200 ppm – which is a typical emission limit for coal-fired power plants [3]. It can be seen that the absorption linewidth of mercury vapor is ~25 GHz, whereas SO_2 has a much broader absorption spectrum without clear structure. Although SO_2 has about one order of magnitude larger absorption, it behaves merely as a broadband light attenuator, consequently, good selectivity can be obtained. The absorption of mercury vapor reaches about 1%, which means that at present the relative noise level is in the order of 10^{-2}. Much better SNR can be expected by utilizing lasers with higher power, and nonlinear frequency conversion materials with improved efficiency.

For the TDLAS technique, at least 80-GHz (three times the absorption linewidth of mercury vapor) of mode-hop-free tuning range is required to extract the whole absorption feature of mercury out of the broadband attenuation due to absorption of other species or particulate scattering [10, 12]. However, for the MDL-COSPEC method, there is no special request on mode-hop-free tuning range; instead, the mode hop is used to increase the wavelength coverage and thus obtain an off-resonant baseline.

#160551 - $15.00 USD Received 3 Jan 2012; revised 3 Feb 2012; accepted 3 Feb 2012; published 13 Feb 2012

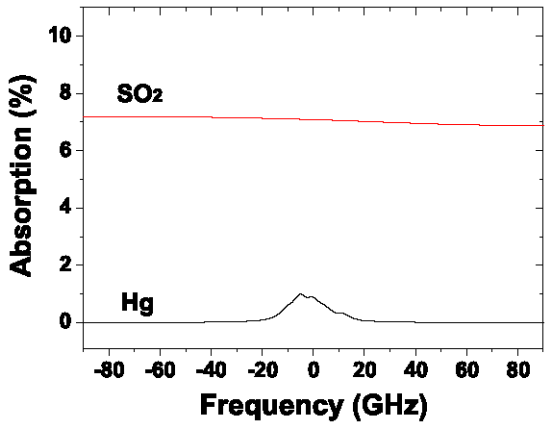

Fig. 9. Simulated spectra of mercury vapor (1 μg/m^3, 1 m) and SO_2 (200 ppm, 1m) at atmospheric pressure.

4.4 Tolerance

An advantage of the MDL-COSPEC technique is the relaxed requirement on wavelength control of the laser source. The tolerance of the present mercury detection system was evaluated by changing the control parameters of the two lasers, including the operating current, temperature, feedback grating angle of the violet diode laser, as well as the operating temperature of the red diode laser, respectively. The initial values of these 4 parameters were 110 mA, 33 °C, 0 rad and 32 °C, respectively. Figures 10(a) and 10(b) show the absorption signals of mercury at different operating currents and temperatures of the violet laser, with the angle of the feedback grating fixed. Since the laser output wavelength in the Littrow-cavity configuration mainly depends on the angle of the feedback grating, even by 40 mA and 8 °C change the output wavelength of the violet laser is mainly constant, and mercury absorption signals can still be readily obtained. The SNR slightly decreases because of the reduced light intensity due to the decrease of the injection current and the mismatch between the emitting laser wavelength and the gain curve center. Figure 10(c) shows the mercury absorption signals at different angles of the feedback grating which were adjusted by a PZT actuator. A change of the grating angle of 8×10^{-5} rad corresponds to ~0.1 nm change of the diffraction wavelength. However, since the wavelength coverage of the red laser is about 1 nm, it is large enough to compensate for the 0.1 nm adjustment of the violet laser. Figure 10(d) shows the absorption signals of mercury at different operating temperatures of the red laser. The 4 °C variance of the red laser temperature yields ~0.5 nm change of the wavelength coverage center, which is less than the total wavelength coverage of 1 nm. Thus gas absorption signals can still be readily obtained. The above tolerance evaluation experiments show that, in contrast to the TDLAS technique, long-term stability and reproducibility of laser modes are no longer prerequisite here because of the employment of a correlation scheme. It is worth noting that the variation range of the parameters performed here does not correspond to some maximum values, but they are large enough to demonstrate the tolerance of the system to laser wavelength changes in practical applications.

#160551 - $15.00 USD Received 3 Jan 2012; revised 3 Feb 2012; accepted 3 Feb 2012; published 13 Feb 2012

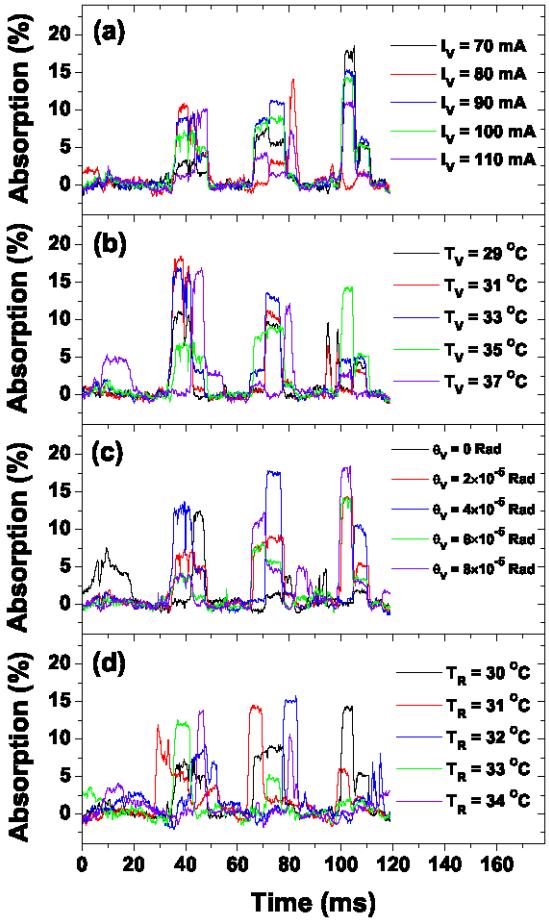

Fig. 10. Mercury absorption signals with different (a) operation currents of the violet DL; (b) temperatures of the violet DL; (c) feedback grating angles of the violet DL; (d) temperatures of the red DL.

5. Conclusions and comments

A gas correlation scheme for elemental mercury detection is demonstrated by using a UV multimode laser source generated by frequency mixing of a violet MDL with a red MDL. Static measurements of mercury vapor are performed at atmospheric pressure and room temperature. A sensitivity of 1 μg/m^2 is achieved with 30-s integration time, which corresponds to a sensitivity of 1 μg/m^3 for 1-m path length. The obtained sensitivity is sufficient for real time monitoring of industrial emissions where typical mercury vapor concentrations are in the order of tens of μg/m^3. For a practical implementation of the sensor, e.g., in mercury emission monitoring from coal-fired utilities, the sampling can be performed by means of a probe where dirt particles are removed prior to analysis and the sample gas is heated to avoid condensation. Adsorption of oxidized mercury by reactive ash may require corrections for low bias in the mercury concentration [5], however, this is beyond the present study.

Although wavelength modulation spectroscopy as a general sensitivity enhancement technique was employed, at present it does not yield advantages over direct absorption detection because of the low power of the UV light. However, much improved sensitivity can be expected by using diode lasers with higher powers and nonlinear materials with improved efficiency. The improved sensitivity can make the system operating with good linearity by filling the gas cells with low concentration gases. MDL-COSPEC can take advantage of the

#160551 - $15.00 USD Received 3 Jan 2012; revised 3 Feb 2012; accepted 3 Feb 2012; published 13 Feb 2012

frequent mode-hop characteristics of the FP type diode lasers to obtain a reference baseline, thus making the system immune to interfering gases such as SO_2, that has a broadband absorption spectrum. Because of employment of a correlation scheme, the system has great tolerance to environmental parameters and laser wavelength changes, which constitutes a promising advantage for real-world applications.

Acknowledgments

This work was supported by a direct Swedish Research Council grant (621-2011-4265), the SIDA-VR Research Link Programme (grant 348-2007-6939), the Natural Science Foundation of China (NSFC) (grant 61008027), and the Fundamental Research Funds for the Central Universities (grant HIT.NSRIF.2009063). G. Somesfalean acknowledges support from the Lund Laser Centre Linnaeus grant. X.T. Lou, G. Somesfalean and Z.G. Zhang are grateful for the Erasmus Mundus External Cooperation Window scholarships from the European Commission.

#160551 - $15.00 USD Received 3 Jan 2012; revised 3 Feb 2012; accepted 3 Feb 2012; published 13 Feb 2012